

Brief Communication



Longitudinal Intravital Imaging of Tumor-Infiltrating Lymphocyte Motility in Breast Cancer Models

Inwon Park ^{1,2}, Sujung Hong ^{3,4}, Joon Seok ⁵, Stephani Edwina Lucia ^{4,5}, Eunjo Song ³, Mingyo Kim ⁶, Eunji Kong ^{4,5}, Howon Seo ^{3,4}, Yoonha Hwang ^{3,4}, Soyeon Ahn ^{3,4}, Seonghye Kim ¹, Dong-Hyun Jang ^{1,2}, Jae Hyuk Lee ^{1,2}, Su-Hyung Park ⁵, Pilhan Kim ^{3,4,5}, You Hwan Jo ^{1,2}

OPEN ACCESS

Received: Apr 30, 2021

Revised: Aug 20, 2021

Accepted: Sep 5, 2021

Correspondence to

You Hwan Jo

Department of Emergency Medicine, Seoul National University Bundang Hospital (SNUBH), 82 Gumi-ro 173beon-gil, Bundang-gu, Seongnam 13620, Korea.
E-mail: drakejo@snuh.org

© 2021 Korean Breast Cancer Society

This is an Open Access article distributed under the terms of the Creative Commons Attribution Non-Commercial License (<https://creativecommons.org/licenses/by-nc/4.0/>) which permits unrestricted non-commercial use, distribution, and reproduction in any medium, provided the original work is properly cited.

ORCID iDs

Inwon Park <https://orcid.org/0000-0001-7525-9189>
Sujung Hong <https://orcid.org/0000-0003-3438-9344>
Joon Seok <https://orcid.org/0000-0002-8016-8385>
Stephani Edwina Lucia <https://orcid.org/0000-0001-9456-1869>
Eunjo Song <https://orcid.org/0000-0003-3597-3593>
Mingyo Kim <https://orcid.org/0000-0003-3744-8522>
Eunji Kong <https://orcid.org/0000-0002-2203-6886>
Howon Seo <https://orcid.org/0000-0003-2983-196X>
Yoonha Hwang <https://orcid.org/0000-0002-0574-1372>

¹Department of Emergency Medicine, Seoul National University Bundang Hospital (SNUBH), Seongnam, Korea

²Department of Emergency Medicine, Seoul National University College of Medicine, Seoul, Korea

³Graduate School of Nanoscience and Technology, Korea Advanced Institute of Science and Technology (KAIST), Daejeon, Korea

⁴KI for Health Science and Technology (KIHST), Korea Advanced Institute of Science and Technology (KAIST), Daejeon, Korea

⁵Graduate School of Medical Science and Engineering, Korea Advanced Institute of Science and Technology (KAIST), Daejeon, Korea

⁶Division of Rheumatology, Department of Internal Medicine, Gyeongsang National University School of Medicine, Jinju, Korea

ABSTRACT

Immunoreactive dynamics of tumor-infiltrating lymphocytes (TILs) within the tumor microenvironment in breast cancer are not well understood. This study aimed to investigate the spatiotemporal cellular dynamics of TILs in breast cancer models. Breast cancer cells were implanted into the dorsal skinfold chamber of BALB/c nude mice, and T lymphocytes were adoptively transferred. Longitudinal intravital imaging was performed, and the spatiotemporal dynamics of TILs were assessed. In the 4T1 model, TILs progressively exhibited increased motility, and their motility inside the tumor was significantly higher than that outside the tumor. In the MDA-MB-231 model, the motility of TILs progressively decreased after an initial increase. TIL motility in the MDA-MB-231 and MCF-7 models differed significantly, suggesting an association between programmed death-ligand 1 expression levels and TIL motility, which warrants further investigation. Furthermore, intravital imaging of TILs can be a useful method for addressing dynamic interactions between TILs and breast cancer cells.

Keywords: Breast neoplasms; Cell movement; Intravital microscopy; Lymphocytes, tumor-infiltrating; Programmed cell death 1 receptor

The introduction of cancer immunotherapy has led to great advances in cancer treatment over the last few decades [1]. Among various therapeutics, adoptive cell therapy (ACT) has been suggested to show an effective immune response towards cancer cells and suppress tumor growth [2]. Throughout the ACT, adoptively transferred immune cells are supposed to facilitate tumor elimination by interacting with cancer cells in the tumor microenvironment [3]. However, due to technical limitations, most evaluations for effective treatment using ACT have focused on the extent and pattern of lymphocyte infiltration using *ex vivo* methods,

Soyeon Ahn 
<https://orcid.org/0000-0002-4955-523X>
 Seonghye Kim 
<https://orcid.org/0000-0002-3869-8008>
 Dong-Hyun Jang 
<https://orcid.org/0000-0002-0277-0987>
 Jae Hyuk Lee 
<https://orcid.org/0000-0003-2429-4085>
 Su-Hyung Park 
<https://orcid.org/0000-0001-6363-7736>
 Pilhan Kim 
<https://orcid.org/0000-0001-8388-1840>
 You Hwan Jo 
<https://orcid.org/0000-0002-9507-7603>

Funding

This work was supported by the Seoul National University Bundang Hospital (SNUBH) research fund (No.14-2020-018) and the National Research Foundation of Korea (NRF) grant funded by the Korea government (MSIT) (NRF-2020R1F1A1058381, NRF-2020R1A2C2013095, NRF-2020R1A2C3005694).

Conflict of Interest

The authors declare that they have no competing interests.

Author Contributions

Conceptualization: Park I, Lee JH, Kim P, Jo YH; Data curation: Park I, Hong S, Seok J, Lucia SE, Kim P; Formal analysis: Park I; Funding acquisition: Park I; Investigation: Park I, Hong S, Seok J, Lucia SE, Kim M, Kong E, Seo H, Hwang Y, Ahn S, Kim S, Jang DH; Methodology: Park I, Song E, Kong E, Seo H, Hwang Y, Ahn S, Kim S, Jang DH; Resources: Song E; Supervision: Lee JH, Park SH, Kim P, Jo YH; Validation: Park SH; Writing - original draft: Park I; Writing - review & editing: Kim M, Kim P, Jo YH.

such as immunohistochemistry or flow cytometry [4,5]. Most studies depend on a simple counting of lymphocyte infiltration, which is presumed to reflect tumor-infiltrating lymphocyte (TIL) activation inside the tumor microenvironment. Previous studies on the motility of TILs [6] provide an improved basis for assessing their activation; however, they are limited to providing information on the motility of lymphocytes in explanted tumor tissues or lymph nodes with an incomplete physiological microenvironment. Therefore, the dynamic behavior of TILs in the tumor microenvironment *in vivo* is unclear [4,5]. Particularly, in breast cancer, where most of the recent trials with immune checkpoint inhibitors have shown discouraging results, the data concerning the dynamic behavior of TILs in breast cancer might provide a new perspective.

To investigate the dynamic behavior of TILs in a breast cancer model *in vivo*, this study utilized an intravital imaging system, comprising a customized video-rate laser scanning confocal microscope to analyze three breast cancer models developed using one mouse (4T1) and two human (MDA-MB-231 and MCF7) cancer cell lines [7,8]. Cancer cells were implanted into the dorsal skinfold chamber of BALB/c nude mice and adoptively transferred T cells that endogenously express the red fluorescence protein DsRed for stable and longitudinal imaging of the dynamic behavior of TILs. We found that the dynamic behavior of TILs was influenced by multiple factors, such as the temporal factors after adoptive T cell transfer, spatial domains in the tissue related to the proximity of T cells with tumors, and types of breast cancer cells.

The detailed methods are described in the **Supplementary Data 1**. BALB/c nude mice (CAN. Cg-Foxn1nu/CrljOri) were purchased from Orient Bio (Suwon, Korea). β -actin-DsRed transgenic mice were used for the adoptive transfer of T lymphocytes. 4T1-Luc2-GFP (referred to as 4T1-GFP) cancer cells were utilized to generate a mouse breast cancer model. MDA-MB-231-GFP and MCF-7-TGL (TK-GFP-Luciferase, referred to as MCF-7-GFP) cancer cells were used to establish human breast cancer models [9]. All invasive surgeries were performed under general anesthesia, and all efforts were made to minimize animal suffering. The experiments with human cancer cell lines were approved by the Institutional Review Board of Seoul National University Bundang Hospital (SNUBH) (protocol No. X-2012/655-902). All animal experiments were conducted following the standard guidelines for the care and use of laboratory animals and were approved by the Institutional Animal Care and Use Committee of Korea Advanced Institute of Science and Technology (protocol No. 2013-30) and SNUBH (protocol No. BA-2012-309-107-01).

The dorsal skinfold chamber was surgically implanted with cancer cells in BALB/c nude mice as described previously [10]. Mouse or human cancer cells (1.0×10^6 cells) were implanted into the dorsal skinfold chamber in mice. Intrinsic DsRed-expressing T lymphocytes were isolated from the spleen of β -actin-DsRed mice and administered to BALB/c nude mice [11]. Isolated T lymphocytes were co-implanted with cancer cells in the 4T1 mouse model and intravenously injected into the MDA-MB-231 and MCF-7 mouse models.

A custom-built laser-scanning intravital confocal microscopy system [12-14] and a commercial intravital confocal microscopy system (IVIM-C; IVIM Technology, Daejeon, Korea) were utilized to visualize the cellular dynamics of TILs in the tumor microenvironment. For motility analysis, time-lapse imaging was performed for each cell for 10 min. Analysis of the track displacement length, track mean velocity, and confinement ratio for TILs and plotting of the track displacement were performed using IMARIS 8.2 (Bitplane,

Zurich, Switzerland) [14,15]. The arrest coefficient is defined as the fraction of the track time that a cell has an instantaneous velocity of less than 2 $\mu\text{m}/\text{min}$ [15,16].

To investigate the dynamic behavior of TILs in the tumor microenvironment of mouse breast cancer over time and location, the 4T1-GFP model was used [9]. With the intravenous transfer of adoptive T cells, only a few T lymphocytes were observed to infiltrate the tumor area, consistent with a previous study [17]. Therefore, for a large number of cell motility analyses, instead of intravenous injection, a mixture of 4T1 mouse cancer (1.0×10^6 cells) and T (1.0×10^7 cells) cells were co-implanted into the dorsal skinfold chamber in mice (**Figure 1A**). From the day of implantation to day 11 post-implantation, the motility of T lymphocytes progressively increased, as determined by the increasing track displacement length, track mean velocity, and

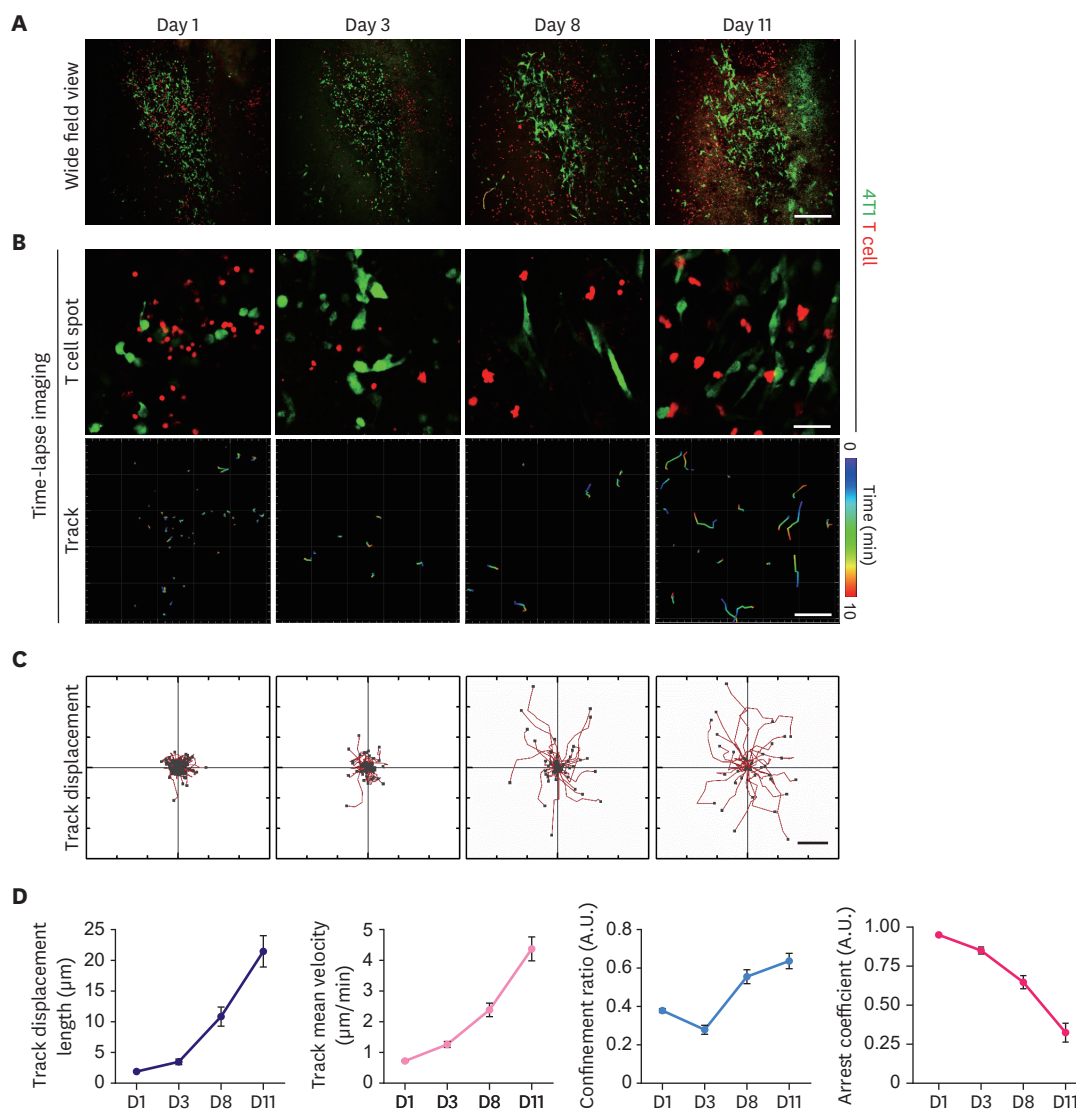


Figure 1. Longitudinal observation of TIL motility in 4T1 murine breast cancer model. (A) Representative wide field view of TILs. Scale bar: 500 μm . (B) Representative time-lapse imaging of TILs. The color-coded track depicts the motion of tracked TILs over a period of 10 minutes (**Supplementary Video 1**). Scale bar: 50 μm . (C) Overlay of the tracks of the TILs recorded by time-lapse imaging. Each TIL track is plotted from the central point and represents XY displacement. Scale bar: 10 μm . (D) Longitudinal trends of track displacement length, track mean velocity, confinement ratio, and arrest coefficient of TILs in 4T1 murine breast cancer model. Data are presented as mean \pm standard error of the mean. D = day; TIL = tumor-infiltrating lymphocyte.

confinement ratio (**Figure 1B-D**, **Supplementary Video 1**). In contrast, the arrest coefficient, which is the proportion of time when a cell is not migrating, gradually decreased, suggesting an increased dynamic behavior of T cells (**Figure 1D**). In addition, cells with increased motility tended to present a highly polarized morphology with lamellipodia at the leading edge of the cell, which is consistent with a previous study [6] (**Supplementary Video 1**). To determine whether programmed death-ligand 1 (PD-L1) expression levels were altered during tumor formation, PD-L1 expression in 4T1 cells in the tumor was assessed using immunofluorescence staining (**Supplementary Figure 1A**) and flow cytometry (**Supplementary Figure 1B**). In both experiments, 4T1 cells showed high levels of PD-L1 expression on day 1, whereas PD-L1 expression levels decreased on day 8.

Thereafter, we hypothesized that the dynamic behavior of TILs in contact with the tumor cells might be different from that of T cells outside the tumor. On day 8, after the adoptive transfer of T cells, when the dynamic behavior of TILs was increasing, the motility of TILs inside and outside the 4T1 tumor was compared to identify the difference in the dynamic behavior of TILs based on their spatial relationship with the tumor (**Figure 2A**). The motility of TIL inside the 4T1 tumor was significantly higher than that outside the 4T1 tumor, as assessed by the increase in the track displacement length, track mean velocity, and confinement ratio (**Figure 2B-C**, **Supplementary Video 2**). Consistently, the arrest coefficient was higher outside the tumor than inside the tumor (**Figure 2C**).

To investigate the motility of TILs in the tumor microenvironment of human breast cancer cells, the MDA-MB-231-GFP model was used [7,8]. For ACT, T lymphocytes (1.0×10^7 cells) were intravenously injected into the tail vein of a cancer cell-implanted mouse [18]. The implementation of the dorsal skinfold chamber and implantation of MDA-MB-231-GFP cells (1.0×10^6 cells) was performed a week before the intravital imaging session (**Figure 3A**).

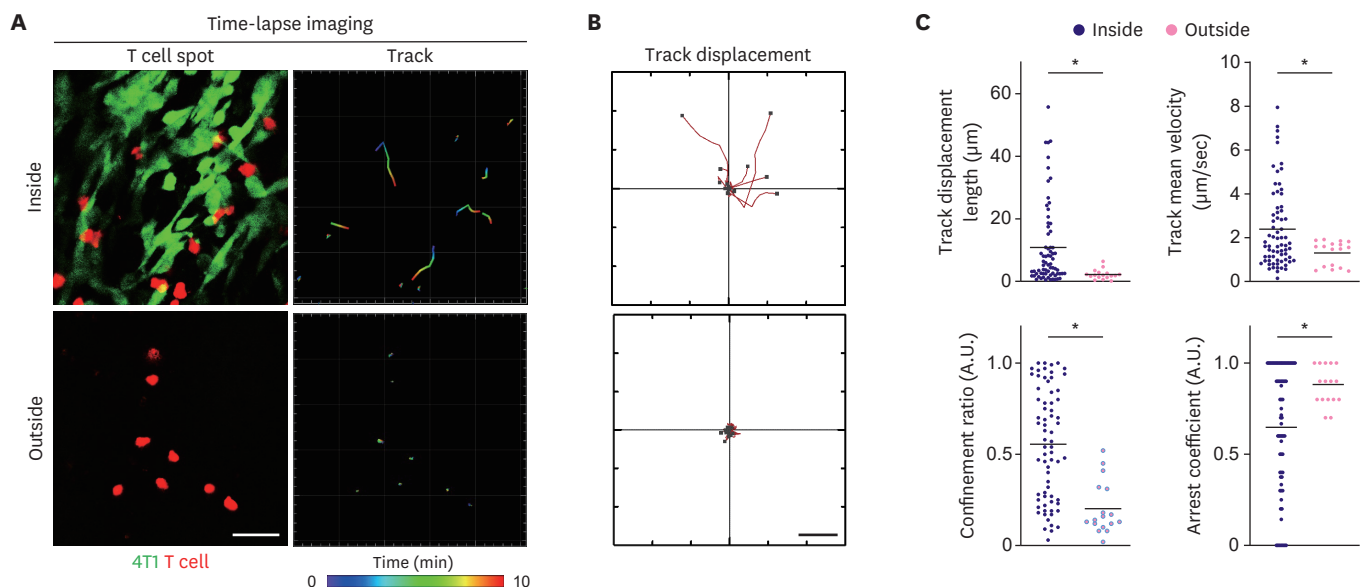


Figure 2. TIL motility at day 8 post implantation in 4T1 murine breast cancer model. (A) Representative time-lapse imaging TILs in the 4T1 murine breast cancer model. The color-coded track describes the motion of tracked TILs over a period of 10 minutes (**Supplementary Video 2**). Scale bar: 50 μm . (B) Overlay of the tracks of TILs recorded by time-lapse imaging. Each TIL track is plotted from the central point and represents XY displacement. Scale bar: 10 μm . (C) Track displacement length, track mean velocity, confinement ratio, and arrest coefficient of TILs inside and outside the 4T1 tumors. Bars represent means.

TIL = tumor-infiltrating lymphocyte.

* $p < 0.05$.

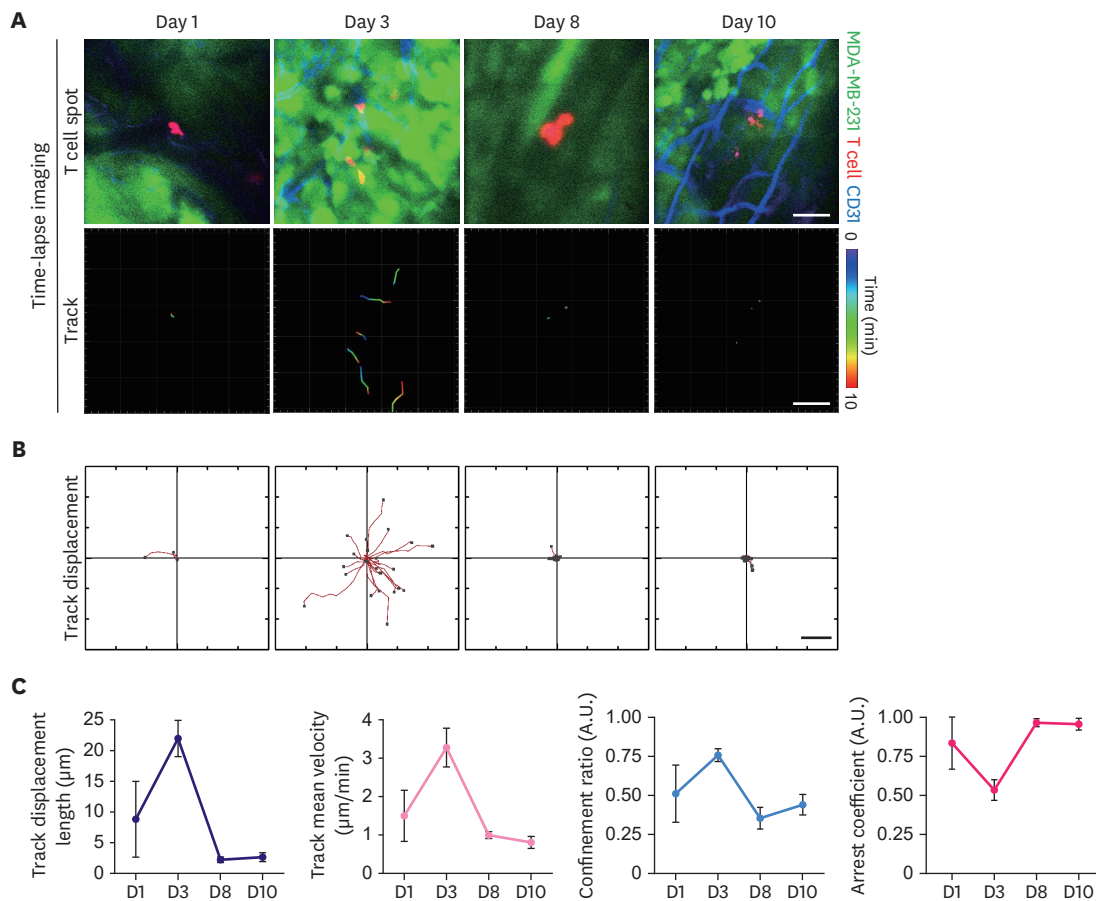


Figure 3. Longitudinal observation of TIL dynamics in MDA-MB-231 human breast cancer model. (A) Representative time-lapse imaging of TILs in the MDA-MB-231 human breast cancer model. The color-coded tracks represent the motion of tracked TILs over a period of 10 minutes (**Supplementary Video 3**). Scale bar: 50 μm . (B) Overlay of the tracks of TILs recorded by time-lapse imaging. Each TIL track is plotted from the central point and represents XY displacement. Scale bar: 10 μm . (C) Longitudinal trends of track displacement length, track mean velocity, confinement ratio, and arrest coefficient of TILs in the MDA-MB-231 human breast cancer model. Data are presented as mean \pm standard error of the mean. D = day; TIL = tumor-infiltrating lymphocyte.

From days 1 to 3 post-adoptive T cell transfer (day 8 to day 10-post cancer cell implantation), the motility of T lymphocytes initially increased but decreased after an increase in the arrest coefficient, suggesting a decreased dynamic behavior of T lymphocytes over time. (**Figure 3A-C**, **Supplementary Video 3**).

To compare with the MDA-MB-231-GFP model, the MCF-7-GFP human breast cancer mouse model was implemented. The different levels of PD-L1 expression in both cancer cells were confirmed by immunofluorescence staining (**Supplementary Figure 2A and B**) and flow cytometry (**Supplementary Figure 2C and D**) [7,8]. On day 8 post-adoptive T cell transfer, which corresponded to day 15 after cancer cell implantation, TILs in MCF-7 moved with a longer displacement length and at higher velocity than in the MDA-MB-231-GFP model (**Figure 4A-C**, **Supplementary Video 4**). The migration trajectories were less restrained, and the arrest coefficients were lower in MCF-7-GFP cells than in MDA-MB-231-GFP cells (**Figure 4D**).

To analyze the changes in the motility of TILs in distinct tumor microenvironments, three different breast cancer models consisting of one mouse (4T1) and two human (MDA-MB-231 and MCF-7) cancer cell lines were utilized. The 4T1 model, which represents a syngeneic

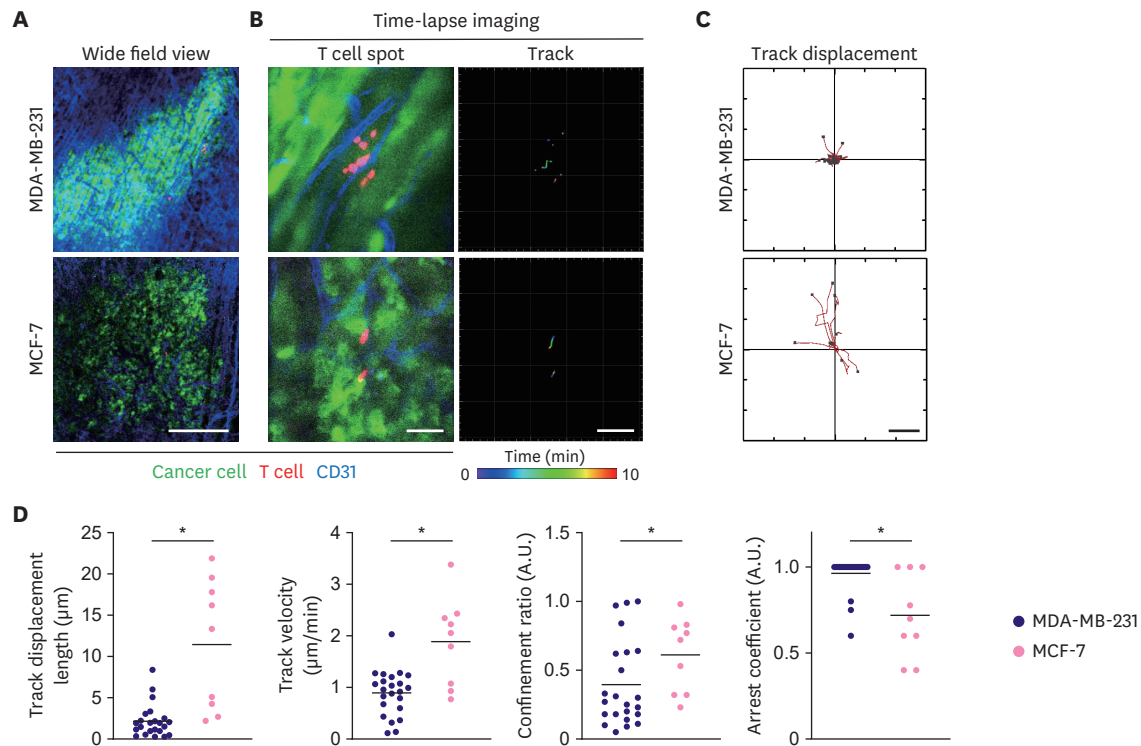


Figure 4. TIL motility in MDA-MB-231 and MCF-7 human breast cancer models at day 15 post implantation. (A) Representative wide field view of TILs in MDA-MB-231 and MCF-7 human breast cancer models. Scale bar: 500 μm . (B) Representative time-lapse imaging of TILs in the MDA-MB-231 and MCF-7 human breast cancer models. The color-coded tracks represent the motion of tracked TILs over a period of 10 minutes (**Supplementary Video 4**). Scale bar: 50 μm . (C) Overlay of the tracks of TILs recorded by time-lapse imaging. Each TIL track is plotted from the central point and represents XY displacement. Scale bar: 5 μm . (D) Track displacement length, track velocity, confinement ratio, and arrest coefficient of TILs in the MDA-MB-231 and MCF-7 human breast cancer models. Bars represent means.

TIL = tumor-infiltrating lymphocyte.

* $p < 0.05$.

murine breast cancer model, demonstrated a progressive increase in TIL motility and decreased PD-L1 expression after cancer cell implantation. However, as only a single type of mouse cancer cell was implemented in our study, several confounding issues such as co-implantation of T cells with cancer cells and tumor formation process remain. Therefore, it cannot be concluded that the increase in TIL dynamics was mainly correlated with the decrease in PD-L1 expression. In addition, although our study with immunofluorescence and flow cytometry indicated that PD-L1 expression was reduced in 4T1 cells 8 days after implantation, controversy over PD-L1 expression in 4T1 cancer cells remains in previous studies (high [19] versus low [9]). Although a spatial correlation of the motility and proximity of TILs to the tumor was evaluated, it cannot be concluded that the motility of TILs is primarily affected by PD-L1 expression, as nearby cancer cells acting as antigens themselves may influence the TILs. Subsequently, human breast cancer cells consisting of two different levels of PD-L1 expression were used to analyze TIL motility in cancer cells with distinct PD-L1 expression; these included the MDA-MB-231 (high PD-L1 expression) and MCF-7 (low PD-L1 expression) cell lines [7,8]. In the xenogeneic human breast cancer model, the motility of TILs in MDA-MB-231 tumors initially increased but soon decreased, which led to arrest-like behavior. In contrast to the TILs in MDA-MB-231 tumors with high levels of PD-L1 expression, TILs in the MCF-7 tumors with low levels of PD-L1 expression showed increased motility. This phenomenon was similarly identified in the TILs in the 4T1 murine breast cancer model 8 days after implantation when the levels of PD-L1 expression were low.

Previous studies have demonstrated the migratory behavior of TILs in the tumor microenvironment, which is debatable [6,16,17]. A study using a murine lung cancer (TC-1) model showed that T lymphocytes migrate randomly within the tumor and become highly motile during tumor regression [6]. Another study using a murine thymoma (EL4 and EG7) model suggested that cytotoxic T lymphocytes in the tumor microenvironment should arrest their migration near antigen-expressing tumors, which is critical for tumor elimination [16]. A study using a murine melanoma (B16) model indicated four different stages of adoptive cytotoxic T lymphocyte migration with varying motilities [17]. Another study using a murine breast cancer (4T1) model showed that monotherapy with an anti-CTLA-4 antibody (9H10) increased the motility of T cells and induced arrest in combination with ionizing radiotherapy [20]. In this study, the motility of T cells was reduced in the high-PD-L1 expression model, suggesting that inhibitory mechanisms might induce T cell arrest. This response may be proposed as T cell exhaustion. However, this study could not identify the clinical effects, such as tumor regression due to technical issues regarding the small number of TILs. Thus, this study attempted to apply human breast cancer cells that showed diverse PD-L1 expression compared with the above studies using a syngeneic murine cancer model.

This study has limitations. T cells were isolated from mice; the T cells might have a reserved immune response to xenogeneic human breast cancer cells, regardless of PD-L1 expression levels. Moreover, different molecular subtypes, including the expression of estrogen receptors between MDA-MB-231 and MCF-7, may be attributed to the dynamics of T cells. Further studies comparing the same molecular subtype of cancer cells with different PD-L1 levels, or cancer cells treated with a PD-L1 inhibitor, may better elucidate the relevant issue. However, as the dynamic behavior of T cells was significantly different between the two human breast cancer models with distinct PD-L1 expression, the existence of PD-L1 as an attributing factor might be one of the hypotheses.

In the syngeneic mouse cancer model (4T1), ACT was applied by co-implantation of T cells with cancer cells, whereas ACT was performed by intravenous injection in human cancer cells (MDA-MB-231 and MCF-7) models. In a preliminary experiment, only a few lymphocytes were observed near cancer cells, limiting the statistical analysis of the dynamics of TILs. Therefore, as a proof-of-concept in intravital imaging studies, we attempted to identify many TIL dynamics in syngeneic mouse cancer cell models that can readily ensure statistical significance. After validating the proof-of-concept in a syngeneic mouse cancer model, we implemented the ACT method in a human cancer cell model to investigate TILs that maximally mimic clinical situations.

In this study, injected T cells differentiated up to the CD8⁺ subtype were not isolated due to a low TIL count during intravital imaging. We attempted to inject 1.0×10^7 untouched pan T cells rather than CD8⁺ T cells as an alternative. Although it was not elucidated in this study, the infiltration of CD8⁺ T cells in breast cancer is an independent favorable prognostic indicator that emphasizes the importance of the composition of CD8⁺ T cells in TILs that exhibit cytotoxic effects [21]. Further intravital imaging studies using CD8⁺ T cells must be considered to confirm that the dynamics of the subtype of TILs in this study were CD8⁺.

Our results suggest that not only the number of TILs in *ex vivo* histology but also their dynamics *in vivo* should be considered to identify the role of TILs in breast cancer. This might also explain the ineffectiveness of immunotherapy in breast cancer reported by previous studies, despite TILs being a prognostic marker in breast cancer [5,22]. Comprehensive studies concerning the functional role of TILs in the tumor microenvironment including cancer cell apoptosis and

further tumor regression may be needed to describe the role of the dynamic behavior of TILs in breast cancer models. In addition, this study could be further developed as an experimental system for monitoring the efficacy of adoptive T cell transfer in breast cancer originating from human patients, such as patient-derived xenograft models [23].

This study achieved *in vivo* visualization of adoptively transferred TILs in mouse and human breast cancer-implanted murine models. We analyzed the dynamic behavior of TILs in mouse and human breast cancer models, including the length, velocity, straightness, and arrest-like behavior, stably and quantitatively using a longitudinal intravital imaging system. Further studies with an identical molecular subtype of cancer cells with siRNA or PD-L1 inhibitors are warranted to prove the hypothesis of correlation between PD-L1 expression and dynamic behavior of TILs. Direct observation of the dynamic behavior of TILs can be highly advantageous for elucidating the mechanisms of the various pathways in breast cancer and evaluating the efficacy of therapeutic candidates targeting programmed cell death protein 1/PD-L1.

ACKNOWLEDGMENTS

The authors would like to thank Prof. Mi-Young Kim (KAIST) and Prof. Joan Massagué (Memorial Sloan-Kettering Cancer Center) for their generous gift of the MCF-7-TGL cells.

SUPPLEMENTARY MATERIALS

Supplementary Data 1

Supplementary Methods

[Click here to view](#)

Supplementary Figure 1

PD-L1 expression level in the 4T1 mouse breast cancer models. (A) Representative immunofluorescence imaging of PD-L1 expression in 4T1 cancer cells at day 1 and 8 post implantation. Scale bar: 100 μm . (B) Flow cytometric analysis of surface expression of PD-L1 on 4T1 cancer cells at day 1 and 8 post implantation.

[Click here to view](#)

Supplementary Figure 2

PD-L1 expression level in the MDA-MB-231 and MCF-7 human breast cancer models. (A) Representative immunofluorescence imaging of PD-L1 expression in MDA-MB-231 and MCF-7 cancer cells at day 15 post implantation. Scale bar: 100 μm . (B) Comparison of PD-L1+ area in MDA-MB-231 and MCF-7 cancer cells. (C) Flow cytometric analysis of surface expression of PD-L1 on MDA-MB-231 and MCF-7 cancer cells at day 15 post implantation. (D) Comparison of gMFI of PD-L1 level in MDA-MB-231 and MCF-7 breast cancer cells.

[Click here to view](#)

Supplementary Video 1

Longitudinal time-lapse imaging of tumor-infiltrating lymphocyte motility in a 4T1 murine breast cancer model. T lymphocytes (red) acquired from Actin-DsRed mice were co-implanted with 4T1 murine breast cancer cells (green) in the dorsal skinfold chamber of BALB/c nude mice. Ten minutes of intravital imaging at 1-min intervals was acquired to identify the dynamic interaction between T lymphocytes (red) and 4T1 cancer cells (green). The scale bar is depicted in the video, and the color bar represents the acquired time of the track of T lymphocytes (1-10 minutes). This video corresponds to the data shown in **Figure 1B and C**.

[Click here to view](#)

Supplementary Video 2

Tumor-infiltrating lymphocyte motility based on tumor location in the 4T1 murine breast cancer model. T lymphocytes (red) acquired from Actin-DsRed mice were co-implanted with 4T1 murine breast cancer cells (green) in the dorsal skinfold chamber of BALB/c nude mice. Ten minutes of intravital imaging at 1-minute intervals was acquired to identify the dynamic interaction between T lymphocytes (red) and 4T1 cancer cells (green). The scale bar is depicted in the video, and the color bar represents the acquired time of the track of T lymphocytes (1-10 minute). This video corresponds to the data shown in **Figure 2A and B**.

[Click here to view](#)

Supplementary Video 3

Longitudinal time-lapse imaging of tumor-infiltrating lymphocyte motility in MDA-MB-231 human breast cancer model. T lymphocytes (red) acquired from Actin-DsRed mice were adoptively transferred via tail vein injection into BALB/c nude mice previously implanted with MDA-MB-231-GFP breast cancer cells (green). Ten minutes of intravital imaging at 1-min intervals was acquired to identify the dynamic interaction between T lymphocytes (red) and MDA-MB-231 cancer cells (green). The scale bar is depicted in the video, and the color bar represents the acquired time of the track of T lymphocytes (1-10 minutes). This video corresponds to the data shown in **Figure 3A and B**.

[Click here to view](#)

Supplementary Video 4

Tumor-infiltrating lymphocyte motility in MDA-MB-231 and MCF-7 human breast cancer models. T lymphocytes (red) acquired from Actin-DsRed mice were adoptively transferred via tail vein injection into BALB/c nude mice previously implanted with MDA-MB-231-GFP or MCF-7 breast cancer cells (green). Ten minutes of intravital imaging at 1-min intervals was acquired to identify the dynamic interaction between T lymphocytes (red) and cancer cells (green). The scale bar is depicted in the video, and the color bar represents the acquired time of the track of T lymphocytes (1-10 minutes). This video corresponds to the data shown in **Figure 4B and C**.

[Click here to view](#)

REFERENCES

1. Kaiser J, Couzin-Frankel J. Cancer immunotherapy sweeps Nobel for medicine. *Science* 2018;362:13.
[PUBMED](#) | [CROSSREF](#)
2. Rosenberg SA, Restifo NP. Adoptive cell transfer as personalized immunotherapy for human cancer. *Science* 2015;348:62-8.
[PUBMED](#) | [CROSSREF](#)
3. Gajewski TF, Schreiber H, Fu YX. Innate and adaptive immune cells in the tumor microenvironment. *Nat Immunol* 2013;14:1014-22.
[PUBMED](#) | [CROSSREF](#)
4. Krummel MF. Illuminating emergent activity in the immune system by real-time imaging. *Nat Immunol* 2010;11:554-7.
[PUBMED](#) | [CROSSREF](#)
5. Salgado R, Denkert C, Demaria S, Sirtaine N, Klauschen F, Pruneri G, et al. The evaluation of tumor-infiltrating lymphocytes (TILs) in breast cancer: recommendations by an International TILs Working Group 2014. *Ann Oncol* 2015;26:259-71.
[PUBMED](#) | [CROSSREF](#)
6. Mrass P, Takano H, Ng LG, Daxini S, Lasaro MO, Iparraguirre A, et al. Random migration precedes stable target cell interactions of tumor-infiltrating T cells. *J Exp Med* 2006;203:2749-61.
[PUBMED](#) | [CROSSREF](#)
7. Xu Y, Wu Y, Zhang S, Ma P, Jin X, Wang Z, et al. A tumor-specific super-enhancer drives immune evasion by guiding synchronous expression of PD-L1 and PD-L2. *Cell Rep* 2019;29:3435-3447.e4.
[PUBMED](#) | [CROSSREF](#)
8. Mittendorf EA, Philips AV, Meric-Bernstam F, Qiao N, Wu Y, Harrington S, et al. PD-L1 expression in triple-negative breast cancer. *Cancer Immunol Res* 2014;2:361-70.
[PUBMED](#) | [CROSSREF](#)
9. Sagiv-Barfi I, Kohrt HE, Czerwinski DK, Ng PP, Chang BY, Levy R. Therapeutic antitumor immunity by checkpoint blockade is enhanced by ibrutinib, an inhibitor of both BTK and ITK. *Proc Natl Acad Sci U S A* 2015;112:E966-72.
[PUBMED](#) | [CROSSREF](#)
10. Lehr HA, Leunig M, Menger MD, Nolte D, Messmer K. Dorsal skinfold chamber technique for intravital microscopy in nude mice. *Am J Pathol* 1993;143:1055-62.
[PUBMED](#)
11. Jensen EC. Use of fluorescent probes: their effect on cell biology and limitations. *Anat Rec (Hoboken)* 2012;295:2031-6.
[PUBMED](#) | [CROSSREF](#)
12. Park I, Choe K, Seo H, Hwang Y, Song E, Ahn J, et al. Intravital imaging of a pulmonary endothelial surface layer in a murine sepsis model. *Biomed Opt Express* 2018;9:2383-93.
[PUBMED](#) | [CROSSREF](#)
13. Park I, Hong S, Hwang Y, Kim P. A novel pancreatic imaging window for stabilized longitudinal *in vivo* observation of pancreatic islets in murine model. *Diabetes Metab J* 2020;44:193-8.
[PUBMED](#) | [CROSSREF](#)
14. Park I, Kim M, Choe K, Song E, Seo H, Hwang Y, et al. Neutrophils disturb pulmonary microcirculation in sepsis-induced acute lung injury. *Eur Respir J* 2019;53:1800786.
[PUBMED](#) | [CROSSREF](#)
15. Beltman JB, Marée AF, de Boer RJ. Analysing immune cell migration. *Nat Rev Immunol* 2009;9:789-98.
[PUBMED](#) | [CROSSREF](#)
16. Boissonnas A, Fetler L, Zeelenberg IS, Hugues S, Amigorena S. *In vivo* imaging of cytotoxic T cell infiltration and elimination of a solid tumor. *J Exp Med* 2007;204:345-56.
[PUBMED](#) | [CROSSREF](#)
17. Qi S, Li H, Lu L, Qi Z, Liu L, Chen L, et al. Long-term intravital imaging of the multicolor-coded tumor microenvironment during combination immunotherapy. *Elife* 2016;5:e14756.
[PUBMED](#) | [CROSSREF](#)
18. Visioni A, Kim M, Wilfong C, Blum A, Powers C, Fisher D, et al. Intra-arterial versus intravenous adoptive cell therapy in a mouse tumor model. *J Immunother* 2018;41:313-8.
[PUBMED](#) | [CROSSREF](#)
19. Lian S, Xie R, Ye Y, Lu Y, Cheng Y, Xie X, et al. Dual blockage of both PD-L1 and CD47 enhances immunotherapy against circulating tumor cells. *Sci Rep* 2019;9:4532.
[PUBMED](#) | [CROSSREF](#)

20. Ruocco MG, Piones KA, Kawashima N, Cammer M, Huang J, Babb JS, et al. Suppressing T cell motility induced by anti-CTLA-4 monotherapy improves antitumor effects. *J Clin Invest* 2012;122:3718-30.
[PUBMED](#) | [CROSSREF](#)
21. Liu S, Lachapelle J, Leung S, Gao D, Foulkes WD, Nielsen TO. CD8+ lymphocyte infiltration is an independent favorable prognostic indicator in basal-like breast cancer. *Breast Cancer Res* 2012;14:R48.
[PUBMED](#) | [CROSSREF](#)
22. Nathan MR, Schmid P. The emerging world of breast cancer immunotherapy. *Breast* 2018;37:200-6.
[PUBMED](#) | [CROSSREF](#)
23. Choi Y, Lee S, Kim K, Kim SH, Chung YJ, Lee C. Studying cancer immunotherapy using patient-derived xenografts (PDXs) in humanized mice. *Exp Mol Med* 2018;50:1-9.
[PUBMED](#) | [CROSSREF](#)